ELSEVIER

Spectrochimica Acta Part A 58 (2002) 673–690

SPECTROCHIMICA ACTA PART A

www.elsevier.com/locate/saa

Ab initio rotation–vibration spectra of HCN and HNC

Gregory J. Harris, Oleg L. Polyansky [1], Jonathan Tennyson *

Department of Physics and Astronomy, University College London, Gower Street, London, WC1E 6BT, UK

Received 13 July 2001; accepted 31 August 2001

Abstract

We have calculated an ab initio HCN/HNC linelist for all transitions up to $J = 25$ and 18000 cm^{-1} above the zero point energy. This linelist contains more than 200 million lines each with frequencies and transition dipoles. The linelist has been calculated using our semi-global HCN/HNC VQZANO + PES and dipole moment surface, which were reported in van Mourik et al. (J. Chem. Phys. 115 (2001) 3706). With this linelist we synthesise absorption spectra of HCN and HNC at 298 K and we present the band centre and band transition dipoles for the bands which are major features in these spectra. Several of the HCN bands and many of the HNC bands have not been previously studied. Our line intensities reproduce via fully ab initio methods the unusual intensity structure of the HCN CN stretch fundamental (00^01) for the first time and also the forbidden (02^20) HCN bending overtone. We also compare the $J = 1 \rightarrow 0$ pure rotational transition dipole in the HCN/HNC ground and vibrationally excited states with experimental and existing ab initio results.

Keywords: Ab initio methods; Potential energy surface; Rotation–vibration spectra

1. Introduction

The infrared spectrum of the HCN/HNC system has been the subject of numerous theoretical and experimental studies and continues to be of great interest to both molecular spectroscopy and astronomy. Within molecular spectroscopy the HCN/HNC system is a prototypical isomerising molecule with stable (HCN) and a metastable (HNC) isomers both with linear geometries. The H nucleus in the bending mode of the molecule undergoes large amplitude motion, so much so that high excitation can result in the H nucleus becoming delocalised and can provide an isomerisation pathway. However, despite many theoretical studies of the isomerising motion of the molecule [1–3] these so called delocalised states have yet to be observed experimentally. The relative simplicity of the HCN/HNC system can provide a benchmark for theoretical analysis which can be extended to more complex molecules. HCN and HNC, are also important molecules throughout astronomy, for example HCN has been observed in comets [4,5], planetary atmospheres [6], molecular clouds [7,8], carbon star atmospheres [9,10] and circumstellar masers

* Corresponding author. Fax: +44-20-7679-2564.
E-mail address: j.tennyson@ucl.ac.uk (J. Tennyson).
[1] Present address: Institute of Applied Physics, Russian Academy of Science, Uljanov Street 46, Nizhnii Novgorod, 603024, Russia.

1386-1425/02/$ - see front matter
PII: S1386-1425(01)00664-3

[11]. In fact, prior to its detection in the interstellar medium in 1971 by the radio astronomers Snyder and Buhl [12,13], HNC had only been observed in the laboratory by means of matrix isolation spectroscopy. Of particular interest to us is the role of HCN in C-star atmospheres, calculations by Jørgensen and co-workers [14,15] suggest that the proper detailed treatment of the vibration–rotation spectrum of HCN can have profound effect on the structure of the C-star model atmospheres. It is this problem that motivated our ongoing project to calculate an extensive ro-vibrational linelist upto high levels of rotational excitation to aid the modelling of these stars.

Much experimental work has been done to measure the intensities and frequencies of both HCN and HNC bands, however, beyond the fundamental bands ab initio intensity calculations have been performed only on the stretching bands of HCN and HNC by Botschwina and co-workers Jakubetz and Lan [2] and Bowman et al. [3] have treated HCN and HNC simultaneously by using semi-global dipole and potential surfaces, to simulate isomerisation and to calculate vibrationally average dipole moments, respectively.

In this work, we present ab initio room temperature (298 K) synthetic spectra for HCN and HNC along with band centres and transition dipoles for the prominent features in the room temperature spectra. We also quote line intensities for the HCN CN stretch fundamental band, which has unusual intensity structure, and also for the forbidden (02^20) bend overtone. These spectra form part of our ongoing work and were calculated from line frequencies and transition dipoles which were computed simultaneously for HCN and HNC using our VQZANO + PES and dipole moment surface (DMS) reported in our earlier work [16]. We also present pure rotational $J = 1 \rightarrow 0$ transition dipoles in the ground and excited states of HCN/HNC.

Ultimately the accuracy of any nuclear motion calculation is dependent upon the accuracy of the preceding electronic structure calculations and the potential and dipole surfaces. It is therefore desirable that we use the best potential and dipole surface that are available to us, in Section 2 we review the merits of existing HCN/HNC PES and DMS. In Section 3, we describe our computational method, in Section 4 we present our spectra and finally we conclude in Section 5.

2. The potential energy and dipole surfaces

Our ongoing project of the calculation of an ab initio HCN/HNC linelist for application in astronomy imposes limits on the type of potential surface that we will be using. At the C-star temperatures in which HCN has a major role in opacity ($T_{\text{eff}} < 3000$ K) [14], a significant amount of HCN/HNC will be in the HNC form. It is also important to note that the transition dipoles of HNC bands are more than twice as strong as the corresponding HCN band transition dipoles, so although HNC will be much less abundant than HCN each HNC molecule will have a larger effect on opacity than each HCN molecule. This makes it desirable to be able to study the behaviour of both HCN and HNC, which requires a global HCN/HNC potential surface that maintains accuracy to high energies.

Wu et al. [17] have fitted a global HCN/HNC potential energy surface (PES) to experimental data to create a PES which can reproduce known experimental vibrational energy levels to within 1 cm^{-1}. However, although spectroscopically fitted surfaces reproduce known experimental data to high accuracy, they tend to extrapolate high lying energy levels outside the fitted region far more poorly than do ab initio surfaces. We intend to perform calculations on HCN/HNC upto 18000 cm^{-1} above the zero point energy (ZPE). At the high end of this range only a few HCN/HNC energy levels have been measured so a fitted PES is likely to perform poorly, for this reason we have chosen to use an ab initio PES.

There are currently three ab initio semi-global HCN/HNC PES available these are the ANO/CCSD(T) PES of Bowman et al. [1], the PES of Varandas and Rodriques [49] and VQZANO + PES covered in an earlier paper [16]. Our ab initio VQZANO + PES simultaneously fits 1527 ANO/CCSD(T) points calculated by Bowman et al. [1] with 242 cc-pCVQZ/CCSD(T) points, the surface is morphed with 17 aug-cc-pCVQZ/CCSD(T) cal-

culated in the HNC region of the PES. Finally to improve the representation of the HNC part of the surface. The VQZANO + surface is also adjusted to coincide with three cc-pCV5Z/CCSD(T) points calculated at the critical points of the HCN/HNC system. The VQZANO + PES includes relativistic and adiabatic corrections, which are often neglected when constructing an ab initio PES.

Vibrational energy level calculations with the VQZANO + PES give stretching band origins that more closely match experiment than do the stretching band origins calculated with the Bowman et al. PES [1] and the bending band origins are of a comparable level of accuracy, see below. The positions of the HCN and HNC minima of the VQZANO + PES are considerably closer to experimental equilibrium bond lengths, determined by isotopic substitution [18,19], than those of the Bowman et al. PES. This is likely to result in the VQZANO + PES giving a better representation of the molecules rotational motion than the Bowman et al. PES. Overall the VQZANO + PES is in general superior to the PES of Bowman et al., as a result we use the VQZANO + PES for the calculations presented here.

There are three semi-global dipole moment surfaces (DMS) available these are the TZP/AQCC DMS of Jakubetz and Lan [2], the aug-cc-pCVTZ/CCSD(T) DMS of Bowman et al. [3] and cc-pCVQZ/CCSD(T) DMS of van Mourik et al. [16]. The DMS of Jakubetz and Lan was calculated with the smallest basis of these three DMS, the intensities calculated with it compare with experiment far less favourably than do our calculations with the van Mourik et al. DMS, see below. The DMS of Bowman et al. [3], uses fewer points and a smaller basis than the van Mourik et al. DMS [16]. The van Mourik et al. surface as a result is the best available DMS and the one which will be employed here.

3. The calculation

Frequencies and dipole transition strengths have so far been calculated for all the HCN/HNC rotational vibrational transitions between states with energy less than 18000 cm^{-1} and $J \leq 25$. This data set contains more than 200 million lines and 80000 rotational vibrational energy levels. Our vibrational, rotational, and dipole transition calculations were performed with the DVR3D program suite [20], which uses an exact kinetic energy (EKE) operator and a discrete variable representation (DVR) for the vibrational motions. Jacobi coordinates were used with Legendre polynomials to give the angular grid points and Morse oscillator-like functions for the radial grids. Thirty-five grid points were used for the R coordinate, 21 for the r coordinate and 50 for the angular coordinate. This basis was optimised to obtain a balance between the level of convergence and the available computer resources. Although this basis is slightly smaller than the one used in our previous work [16], it is sufficient to converge all calculations reported here. The parameters for the morse oscillator like basis in the r coordinate are $r_e = 2.3\ a_0$, $D_e(r) = 29.0\ E_h$ and $\omega_e(r) = 0.0105\ E_h$. The parameters for the morse oscillator like basis in the R coordinate are $R_e = 3.2\ a_0$, $D_e(R) = 5.0\ E_h$ and $\omega_e(R) = 0.004\ E_h$. Where r_e is the equilibrium distance, D_e is the dissociation energy and ω_e is the harmonic frequency, see Ref. [20].

The huge number of lines that we have calculated required a large amount of processing power which make it necessary to parallelise the processor intensive routines of the DVR3D codes. The openMP fortran API multiprocessing directives [21] with the MIPSpro 7 Fortran 90 compiler [22] on the 'Miracle' 24 processor SGI Origin 2000 computer, were used to perform the parallelisation. The most processor intensive module of the DVR3D suite is DIPOLE3, which calculates dipole transition strengths between states which are not rigorously dipole forbidden. One loop of this module calls a rank 1 matrix update subroutine and consumes 95% of the runtime. By parallelising this loop we were able to reduce the run time by a factor of five when running on eight processors.

We have used our linelist to calculate room temperature (298 K) absorption spectra of both HCN/HNC and HNC as a separate molecule. The spectral calculations were limited to bands which have lines with absolute intensity above 4

$cm^{-1}\,mol^{-1}$. Figs. 1 and 2 show a spectral map of the HCN/HNC spectrum over the range 0–18000 cm^{-1}, the intensity of HNC bands at room temperature is less than the cut off intensity, so there are no HNC bands shown in this spectrum. Fig. 3 show the spectrum in the region of the (40^00) stretching overtone.

To ease comparison with experiment and earlier ab initio work, the line transition dipole data was reduced to band transition dipoles for all the HCN bands shown in the spectrum and for other selected bands, see Tables 1 and 2. For a given band this was done by dividing each line transition dipole by the square root of the appropriate Hönl-London and vibrational intensity factors to give the band dipole for that line. The mean band dipole and the standard deviation were calculated using the band dipole calculated from each line. Our standard deviation thus measures the reliability of using band dipoles and Hönl-London factors, it does not account for the systematic errors in our calculation.

The Hönl-London factors used in experimental works by two different groups, Maki et al. [23] and Smith et al. [24] differ by a constant in some cases. Van Mourik et al. [16] re-derived the Hönl-London factors from the matrix elements given by Gordy and Cook [25] and they agree with the Hönl-London factors of Maki et al. In all cases we have used the Hönl-London and vibrational factors of Maki et al. and in the cases where we have used the data of Smith et al. we have converted from their Hönl-London factors to those of Maki et al.

For a band with unusual or perturbed structure it is more meaningful to compare line intensities directly than it is to compare fitted band dipoles and Herman–Wallis constants. For this reason two bands for which band transition dipoles are inappropriate are not included in the band dipole table. These bands are the HCN C–N fundamental (00^01) (see Table 3) which has unusual R branch structure, see Maki et al. [26], and the

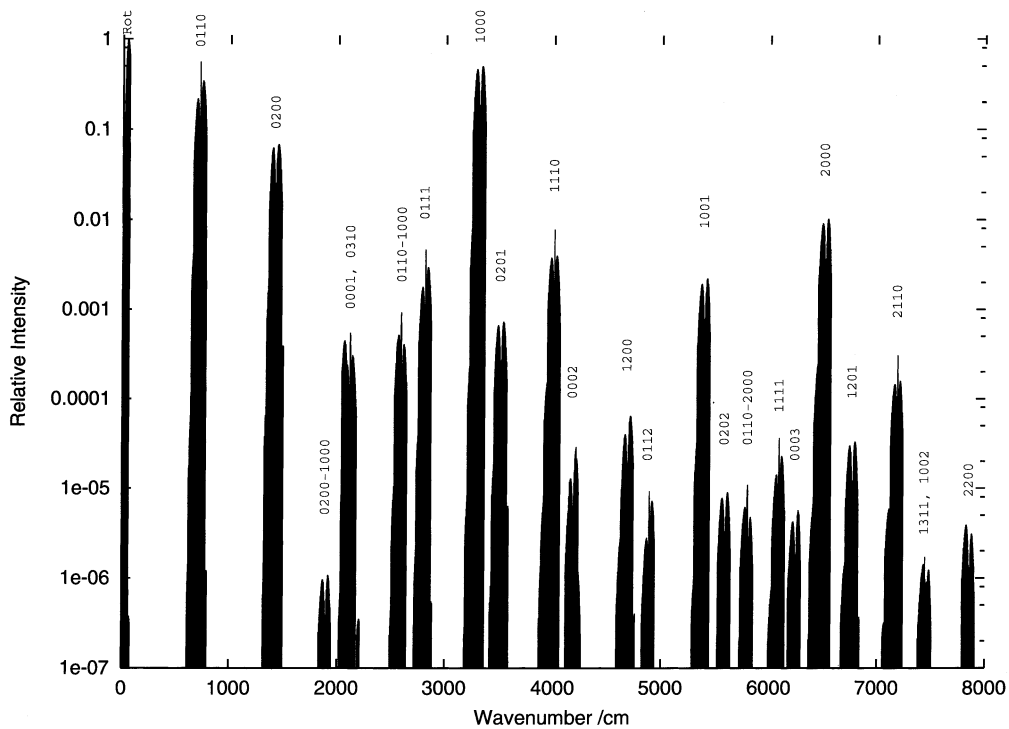

Fig. 1. Ab initio spectral atlas for HCN in absorption, between 0 and 8000 cm^{-1} at 298 K. transitions are labelled $v'_1v'_2l'v'_3$ for transitions from the ground state and $v'_1v'_2l'v'_3 - v''_1v''_2l''v''_3$ for transitions from an excited state.

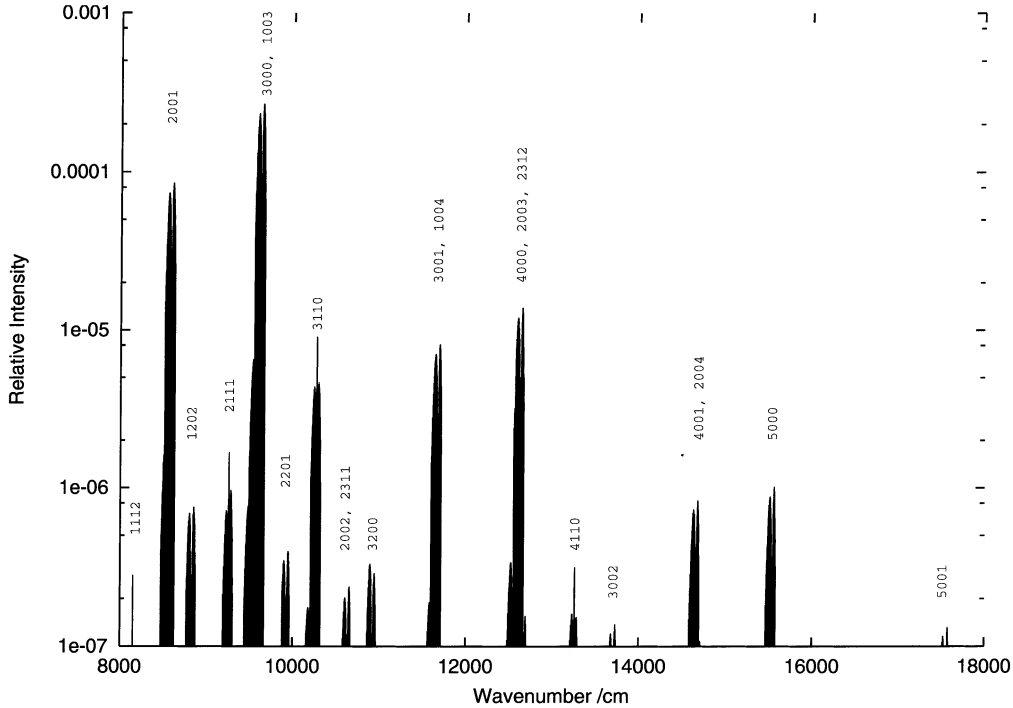

Fig. 2. Ab initio spectral atlas for HCN in absorption, between 8000 and 18000 cm^{-1} at 298 K. transitions are labelled $v'_1v'_2l'v'_3 - v''_1v''_2l''v''_3$ for transitions from an excited state.

forbidden HCN bend overtone (02^20) (see Table 3). For these bands we compare our calculated absolute lines intensities with experimental absolute line intensities. Line intensity can be calculated from line transition dipole by using:

$$I_L = \frac{2\pi^2 L\upsilon(2J''+1)}{3hc\varepsilon_0 Q_{\mathrm{vr}}}\left(\frac{273.15}{T}\right)\exp\left(\frac{-E''}{kT}\right)\left[1-\exp\left(\frac{-hcv}{kT}\right)\right]\mu_L^2 \quad (1)$$

Here, for clarity we use SI units where possible, I_L is the line intensity ($m^{-2}\,atm^{-1}$), L is the Loschmidt number (2.686763×10^{25} molecules m^{-3} at 1 atm and 273.15 K), v is the wavenumber in m^{-1} of the line, h is the Planck constant, c is the speed of light, ε_0 is the permittivity of free space, k is the Boltzmann constant, E'' is the energy of the lower ro-vibrational energy level, T is the temperature, Q_{vr} is the ro-vibrational partition function and μ_L is the line transition dipole in coulomb meters (1 debye $= 3.33564\times10^{-30}$ C m). For the particular combination of units of dipole moment in Debye, intensity in $cm^{-2}\,atm^{-1}$ and wavenumber in cm^{-1}, Eq. (1) becomes:

$$I_L = \frac{11.183309\times v(2J''+1)}{Q_{\mathrm{vr}}}\left(\frac{273.15}{T}\right)\exp\left(\frac{-E''}{kT}\right)\left[1-\exp\left(\frac{-hcv}{kT}\right)\right]\mu_L^2 \quad (2)$$

In this work a value of $Q_{\mathrm{vr}}(298\ \mathrm{K}) = 149.944$ given by Maki et al. [33] was used.

The experimental data of Smith et al. [24,27,28] and the earlier theoretical work of Botschwina and co-workers [29–31], was originally reported as integrated band intensities ($cm\,mol^{-1}$). For consistency we have converted these band intensities to band transition dipoles. Band intensity is related to band transition dipole by the formula:

$$I_{\mathrm{B}} \approx \frac{2\pi^2 N_{\mathrm{A}} v_0}{3hc\varepsilon_0}\left[1-\exp\left(\frac{-hcv_0}{kT}\right)\right]\mu^2 \quad (3)$$

Again for clarity we use SI units, where I_{B} is the band intensity in $m\,mol^{-1}$, N_{A} is the Avogadro number, v_0 is the wavenumber in m^{-1} of the band

centre and μ is the transition dipole in C m. This formula is based upon Eq. (1) and takes into account the manipulation that Smith et al. [24] performed on their data to give integrated band intensities. The approximation here is a result of using the wavenumber of the band centres rather than that of the individual lines. At worst this approximation is accurate to a few percent, better than the approximation made when using Hönl-London factors and less than the experimental statistical error. The factor in square brackets on the RHS of Eq. (3) is the population difference between the two states. It gives rise to induced emission and is very close to 1 for the range of results reported in this work. With rearrangement and using the particular combination of units of dipole moment in Debye, intensity in cm mol^{-1} and wave number in cm^{-1}, the above formula becomes:

$$\mu \approx \sqrt{\frac{I_B}{2.5066379 \times 10^5 \times \nu_0}} \quad (4)$$

This equation is of the same form as used by Botschwina et al. [29], to convert between band transition dipole and band intensity.

The aim of our calculations is to produce a complete linelist of the HCN/HNC system including transitions to and from HCN, HNC and the delocalised states. Consequently localised HCN and HNC transitions are mixed together with the delocalised states. To produce a room temperature HNC only spectrum it is necessary to separate the localised HNC transitions from the other transitions. Bowman et al. [3] have suggested using the sign of the permanent dipole moment of a vibrational level to identify it as a HCN or HNC state. It is difficult to obtain absolute information from our calculated transition dipoles, so in this work HNC and HCN states are separated by comparing the transition dipole of a ro-vibrational state to the ground HCN state and to the ground HNC state. Localised HNC states will have a far greater transition dipole to the HNC

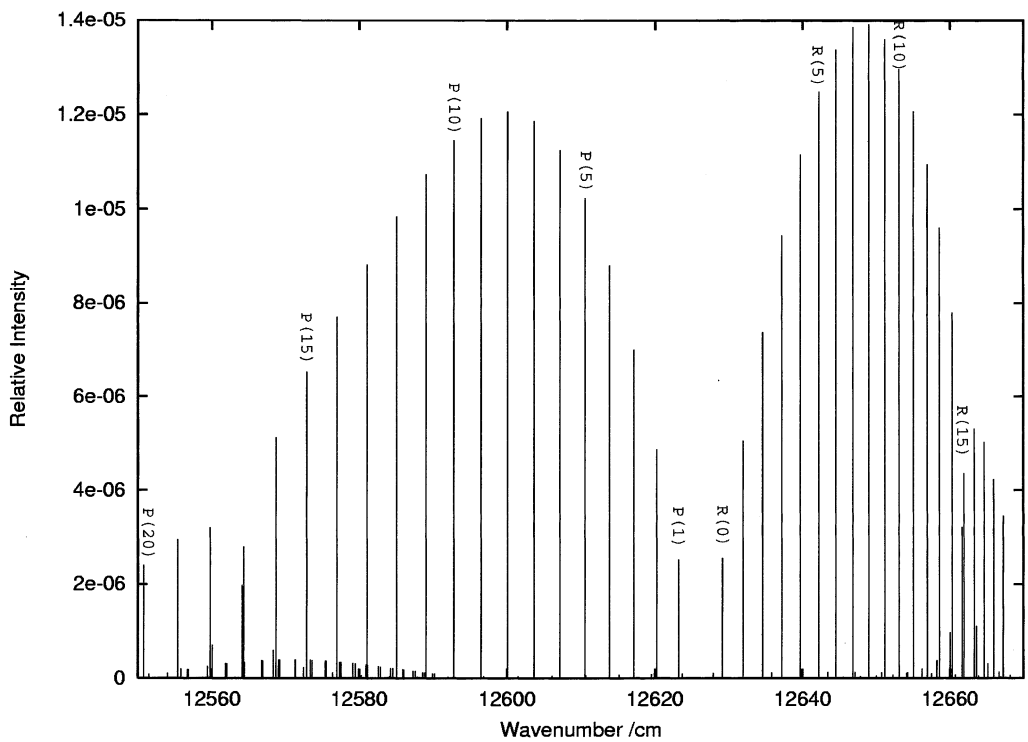

Fig. 3. Absorption spectrum in the region of the HCN (40^00) overtone at 298 K. The HCN (40^00) overtone shows a significant dip in intensity as a result of intensity borrowing in the region of the $J'' = 17$ P branch line and the $J'' = 15$ R branch line.

Table 1
A comparison of experimental and theoretical band centres and transition dipoles for the most prominent HCN bands at 298 K that have excitation in the bending mode, in cm^{-1} and Debye and standard deviation in the last digit given in brackets

$v'_1v'_2l'v'_3$	$v''_1v''_2l''v''_3$	Experiment[a]		This work[b]	
		v_0	μ	v_0	μ
0 4 2 0	0 3 1 0	674.414		668.30	0.184(3)
0 3 1e 0	0 2 2 0	686.921	0.188(1)	682.13	0.175(13)
0 3 1f 0	0 2 2 0	686.921	0.189(1)	682.22	0.202(11)
0 4 0 0	0 3 1 0	689.509	0.185(3)	687.10	0.196(26)
0 2 0 0	0 1 1 0	699.434	0.183(5)	699.03	0.199(17)
0 3 1 0	0 2 0 0	702.037	0.190(2)	699.50	0.197(8)
0 4 2e 0	0 3 1 0	704.725	0.196(5)	702.91	0.187(31)
0 4 2f 0	0 3 1 0	704.725	0.188(7)	703.00	0.196(4)
0 1 1 0	0 0 0 0	711.980	0.189(1)	715.93	0.200(1)
0 2 2e 0	0 1 1 0	714.550	0.189(4)	716.30	0.196(17)
0 2 2f 0	0 1 1 0	714.550	0.188(4)	716.35	0.200(2)
0 3 3e 0	0 2 2 0	717.231	0.196(1)	716.87	0.198(5)
0 3 3f 0	0 2 2 0	717.231	0.197(1)	716.87	0.198(6)
0 4 4e 0	0 3 3 0	720.021		718.22	0.198(5)
0 4 4f 0	0 3 3 0	720.021	0.201(5)	718.22	0.198(5)
0 4 2e 0	0 2 2 0	1391.65	0.0486(2)	1385.12	0.0470(14)
0 4 2f 0	0 2 2 0	1391.65	0.0488(2)	1385.12	0.0475(12)
0 4 0 0	0 2 0 0	1391.56	0.0489(2)	1386.55	0.0470(10)
0 3 1e 0	0 1 1 0	1401.47	0.0471(2)	1398.43	0.0496(35)
0 3 1f 0	0 1 1 0	1401.47	0.0475(4)	1398.57	0.0463(32)
0 2 0 0	0 0 0 0	1411.41	0.0496(2)	1414.92	0.0479(11)
1 0 0 0	0 2 0 0	1900.06		1892.83	0.00498(7)
0 4 0 0	0 1 1 0	2090.98	0.00320(1)	2085.62	0.00369(50)
0 4 2e 0	0 1 1 0	2106.20	0.00330(2)	2101.43	0.00342(65)
0 4 2f 0	0 1 1 0	2106.20	0.00327(1)	2101.48	0.00357(14)
0 3 1 0	0 0 0 0	2113.45	0.003263(1)	2114.46	0.00359(15)
1 2 0 0	0 3 1 0	2570.86	0.0228(1)	2571.81	0.0236(14)
1 1 1e 0	0 2 2 0	2577.63	0.0232(1)	2571.98	0.0229(17)
1 1 1f 0	0 2 2 0	2577.63	0.0232(1)	2572.03	0.0245(15)
1 1 1 0	0 2 0 0	2592.75	0.0226(1)	2589.31	0.0239(24)
1 0 0 0	0 1 1 0	2599.50	0.0226(1)	2591.75	0.0238(10)
0 1 1 1	0 0 0 0	2807.06	0.00824(5)	2813.98	0.00906(36)
0 2 0 1	0 0 0 0	3502.12		3510.99	0.00313(6)
1 1 1 0	0 0 0 0	4005.63	0.00986(11)	4004.27	0.00986(94)
1 3 1e 0	0 1 1 0	4654.89	0.000784(3)	4650.21	0.000785(110)
1 3 1f 0	0 1 1 0	4654.89	0.000786(4)	4650.34	0.000781(80)
1 2 0 0	0 0 0 0	4684.31	0.000795(5)	4686.28	0.000735(93)
0 1 1 2	0 0 0 0	4879.73		4891.88	0.000310(51)
0 2 0 2	0 0 0 0	5571.89		5586.50	0.000272(3)
2 0 0 0	0 1 1 0	5806.15	0.00137(1)[c]	5797.45	0.00172(8)
1 1 1 1	0 0 0 0	6084.80	0.00052(4)[c]	6088.56	0.000545(19)
2 2 0 0	0 2 0 0	6441.54	0.00892(14)	6440.92	0.00789(1)
2 1 1e 0	0 1 1 0	6480.78	0.00889(4)	6474.62	0.00835(22)
2 1 1f 0	0 1 1 0	6480.78	0.00901(4)	6474.71	0.00826(6)
1 2 0 1	0 0 0 0	6761.33		6768.51	0.000479(7)
2 1 1 0	0 0 0 0	7194.22		7190.60	0.00146(12)
1 3 1 1	0 0 0 0	7440.48		7445.62	0.000107(8)
2 2 0 0	0 0 0 0	7853.51		7855.83	0.000150(20)
1 1 1 2	0 0 0 0			8182.18	$4.14(6)\times10^{-5}$
2 1 1 1	0 1 1 0	8544.07	0.00071(5)[c]	8543.75	0.000625(4)

Table 1 (*Continued*)

$v'_1v'_2l'v'_3$	$v''_1v''_2l''v''_3$	Experiment[a]		This work[b]	
		v_0	μ	v_0	μ
1 2 0 2	0 0 0 0	8816.00		8830.27	$6.35(10)\times10^{-5}$
2 1 1 1	0 0 0 0	9257.53	$8.2(6)\times10^{-5}$ [c]	9259.64	$9.48(19)\times10^{-5}$
3 1 1 0	0 1 1 0	9568.35	0.0010(4)[c]	9560.81	0.001082(9)
2 2 0 1	0 0 0 0	9914.40	$5.5(2)\times10^{-5}$ [c]	9922.92	$4.31(2)\times10^{-5}$
3 1 1 0	0 0 0 0	10281.8	$3.2(2)\times10^{-5}$ [c]	10 276.7	0.000210(19)
2 3 1 1	0 0 0 0			10580.5	$1.43(15)\times10^{-5}$
3 2 0 0	0 0 0 0			10 925.2	$3.78(28)\times10^{-5}$
4 1 1 0	0 1 1 0	12557.3	0.00023(3)[c]	12 548.1	0.000218(5)
2 3 1 2	0 0 0 0			12 624.3	$1.55(1)\times10^{-6}$
4 1 1 0	0 0 0 0	13270.8	$1.4(4)\times10^{-5}$ [c]	13 264.1	$3.47(42)\times10^{-5}$
5 1 1 0	0 1 1 0	15452.1	$6.6(5)\times10^{-5}$ [c]	15 441.0	$5.32(6)\times10^{-5}$
5 1 1 0	0 0 0 0	16165.6	$3.4(3)\times10^{-5}$ [c]	16 156.9	$6.67(115)\times10^{-6}$ [d]

[a] Experimental data, band centres taken from Refs. [27,34,43–45], transition dipoles from Maki et al. [23] and from Smith et al. [24,27] where marked.

[b] The ab initio calculations of this work, using the VQZANO + PES and the cc-pCVQZ/CCSD(T) DMS of van Mourik et al. [16].

[c] Experimental measurements of Smith et al. [24,27].

[d] This band is involved in intensity stealing.

ground state than to the HCN ground state. This allowed us to identify localised HNC energy levels and transitions between them. Using this method only a handful of HCN states were mis-identified as HNC states, these tended to be HCN states with extremely low transition dipoles to the ground state, for example the HCN bending overtone $(08^80)\leftarrow(00^00)$ which is a forbidden transition. Transitions involving these few miss-identified states were removed by hand. It may also be possible to identify delocalised states using this method. The wave functions of delocalised states have significant magnitude in both HCN and HNC potential wells and so should have similar transition dipole to the low lying localised states. However, as a result of the problems discussed above this is a qualitative method and is not wholly reliable.

We are in the process of calculating a fully ab initio partition function, but at present despite our literature searches we have not found a partition function for HNC. This effects only calculation of absolute intensities for HNC and will not effect our spectra in which we give relative intensities or our band transition dipoles.

Fig. 5 shows a spectral map of HNC in absorption for 0–8000 cm^{-1}, Fig. 6 is the absorption spectrum in the region of the Q and R branch of the bending fundamental. Band transition dipoles for the prominent HNC bands are compared with existing experimental and theoretical values in Tables 5 and 6.

Finally from the $J=0\rightarrow1$ pure rotational transitions in the HCN and HNC ground and some HCN excited states, we give vibrationally averaged permanent dipoles and compare them with experiment and the ab initio vibrationally averaged dipole moments calculated by Bowman et al. [3], see Table 7.

The vibrationally averaged dipole moment of a given state is approximately equal to the $J=0\rightarrow1$ pure rotational transitions from the following argument. The rotational transition dipole moment for a given vibrational level n is given by: $\langle nJ'|\underline{\mu}|nJ''\rangle$. The vibrationally averaged dipole moment is the case where $J'=J''=0$ and can be approximately equated to the rotational transition dipole multiplied by the correct Hönl-London factor:

$$\langle n0|\underline{\mu}|n0\rangle \approx \langle nJ'|\underline{\mu}|nJ''\rangle H_J \quad (5)$$

Furthermore $H_J=1$ for the case where $J'=1$ and $J''=0$. Therefore the $J=1\rightarrow0$ pure rotational transition dipole is equal to the vibrationally averaged dipole moment within the approximations made when using Hönl-London factors.

Table 2
A comparison of experimental and theoretical stretching band centres and transition dipoles for some of the most prominent HCN stretching bands at 298 K, in cm^{-1} and Debye ($\times 10^{-3}$), with standard deviation in the last digit given in brackets

$v'_1v'_2l'v'_3$	$v''_1v''_2l''v''_3$	Experimental[a]		This work[b]		Earlier ab initio work		
		v_0	μ	v_0	μ	ANO[c] v_0	μ_{GTO}[d]	μ_{AQCC}[e]
1 0 0 0	0 0 0 0	3311.48	83.1(17)	3307.75	85.3(16)	3334.1	83.4	0.0703
0 0 0 2	0 0 0 0	4173.07		4181.45	0.466(52)[f]	4161.5	0.130	0.773
1 0 0 1	0 0 0 0	5393.70		5394.43	4.37(2)	5399.4	4.63	2.41
0 0 0 3	0 0 0 0	6228.60	0.12(2)[g]	6242.42	0.198(12)	6211.4	0.117	0.247
2 0 0 1	0 0 0 1	6488.74	8.7(3)	6484.16	8.49(3)			
2 0 0 0	0 0 0 0	6519.61	8.81(12)	6513.50	8.60(4)	6553.2	8.78	5.22
1 0 0 2	0 0 0 0	7455.42	0.11(1)[g]	7461.58	0.0959(91)	7445.7	0.0974	0.245
2 0 0 1	0 0 0 0	8585.58	0.68(1)[g]	8584.59	0.677(4)	8595.9	0.785	0.468
1 0 0 3	0 0 0 0	9496.44	0.066(3)[g]	9508.91	0.0648(8)	9474.5	0.0771	0.0796
3 0 0 0	0 0 0 0	9627.09	1.03(2)[g]	9619.20	1.138(6)	9668.3	1.12	1.11
2 0 0 2	0 0 0 0	10631.4	0.050(2)[g]	10636.8	0.0320(4)	10 623.7	0.0614	0.0229
1 0 0 4	0 0 0 0	11516.6		11536.1	0.0114(7)	11 487.4		
3 0 0 1	0 0 0 0	11674.5	0.185(4)[g]	11672.2	0.179(5)	11 686.9	0.202	0.283
4 0 0 0	0 0 0 0	12635.9	0.222(7)[g]	12626.2	0.225(2)[f]	12 686.1		
2 0 0 3	0 0 0 0	12658.0	0.053(4)[g]	12669.9	0.0239(5)	12 638.6		
3 0 0 2	0 0 0 0	13702.2	0.029(2)[g]	13708.5	0.0216(1)	13 695.5	0333	0.0499
2 0 0 4	0 0 0 0	14653.7	0.048(2)[g]	14685.0	0.0187(6)	14 642.8		
4 0 0 1	0 0 0 0	14670.5	0.051(2)[g]	14656.9	0.0513(3)	14 683.9		
5 0 0 0	0 0 0 0	15551.9	0.067(8)[g]	15539.3	0.0550(5)	15 604.1	0.0671	0.165
3 0 0 3	0 0 0 0	15710.5	0.0036(4)[g]	15721.7	0.00487(3)[f]	15 700.3	0.00730	0.00196
2 0 0 5	0 0 0 0	16640.3	0.0098(6)[g]	16660.7	0.00793(17)	16 634.5		
4 0 0 2	0 0 0 0	16674.2	0.0202(8)[g]	16685.0	0.00786(20)	16 683.6		
5 0 0 1	0 0 0 0	17550.4	0.0282[h]	17551.0	0.0154(58)[f]	17 574.4	0.0286	0.0755

[a] Experimental data, band centres taken from Refs. [27,34,43–45], transition dipoles from Maki et al. [23] and others where marked.

[b] The ab initio calculations of this work, using the VQZANO + PES and the cc-pCVQZ/CCSD(T) DMS of van Mourik et al. [16].

[c] The ab initio ANO/CCSD(T) vibrational energy level calculations of Bowman et al. [1].

[d] The ab initio 110 cGTO stretch only HCN DMS and calculations of Botschwina et al. [29], Botschwina et al. also calculated a combined intensities for three pairs of strong stretching bands: (40^00) and (20^03), (20^04) and (40^01), (20^05) and (40^02), see text.

[e] The ab initio TZP AQCC semi-global DMS and calculations of Jakubetz and Lan [2], using the Bowman et al. [1] potential surface.

[f] These bands are involved in intensity stealing.

[g] Measurements of Smith et al. [24,27].

[h] Measurement from Romanini and Lehmann [28].

4. Results and discussion

4.1. HCN spectrum

Overall for transitions involving the lower energy levels ($< 10000\ cm^{-1}$) the transition dipoles of our bands (see Tables 1 and 2) agree in most cases to within combined errors with experimental work and the ab initio work of Botschwina et al. [29]. However, for transitions involving the higher energy levels ($> 10000\ cm^{-1}$) there are more significant deviations from experiment with five band dipoles differing from experiment by a factor of two. These transitions are (20^03), (31^10), (41^10), (20^04) and (40^02). There appears to be something anomalous about the (31^10) measurement which is not reproduced by our calculations which predict that ($n1^10$) should have $\mu \sim 10^{-(n+1)}D$ and agree well with experiment and theory for $n = 1, 2, 4, 5$. The stretching combination bands (20^03), (20^04) and (40^02) each lie within $40\ cm^{-1}$ of a strong stretching

combination band, these bands forming a pair of bands which interact, the band pairs being: (40^00) and (20^03), (20^04) and (40^01), (20^05) and (40^02). The difference between the band centres of each band pair in our calculations tends to differ from experiment by about 10 cm^{-1}, this will serve to increase or decrease the interaction between the bands in each pair depending on whether the bands are closer together or further apart. The individual band intensities of these pairs of bands have not been reproduced accurately via fully ab initio techniques. Indeed Botschwina et al. [29] who used a smaller 130 cGTO basis HCN stretching PES and 110 cGTO basis DMS, sidestepped the problem by calculating combined band intensities for each pair. To accurately reproduce experiment for these interacting bands, very accurate wave functions are needed, as was shown by Botschwina [30] who reproduced experiment more accurately by using an empirical correction to his wavefunctions.

Overall our calculations agree to a similar level of accuracy as the calculations of Botschwina et al. [29] and agree more closely to experiment in the case of the (30^03) overtone from which the dipole from Botschwina deviates by a factor of two. It must be stressed that the calculations of Botschwina et al. involve only two-dimensional HCN stretching coordinates and use two-dimensional potential and dipole functions only and give no information on bending excitations. Our band transition dipoles are significantly better than the AQCC calculations of Jakubetz and Lan [2] supporting our choice of dipole surface.

There are two bands in our spectrum which have not yet been experimentally identified and may well be experimentally detectable, these are (11^12) ← (00^00) and (23^11) ← (00^00). There is an element of intensity borrowing present in some bands, one particular example is the (40^00) ← (00^00) band, see Fig. 3. This band shows a significant dip in intensity as a result of intensity borrowing by the (23^12) ← (00^00) band in the re-

Table 3
A comparison of experimental and theoretical line intensities ($cm^{-2}\,atm^{-1}\times10^{-3}$) for the HCN ($00^01$) fundamental band

P branch		J''	R branch	
Experimental[a]	This work		Experimental[a]	This work
		0	0.193	0.323
0.337	0.487	1	0.300	0.497
0.839	1.14	2	0.295	0.541
1.36	1.92	3	0.236	0.497
2.03	2.81	4	0.171	0.385
2.87	3.75	5	0.0725	0.256
	4.71	6	0.0161	0.133
4.23	5.61	7		0.0445
4.97	6.44	8	0.0297	0.00249
5.55	7.08	9	0.124	0.0124
5.86	7.53	10	0.222	0.0705
6.11	7.80	11	0.358	0.167
6.09	7.85	12	0.506	0.288
6.00	7.70	13	0.670	0.420
5.84	7.37	14	0.796	0.544
5.46	6.91	15	0.910	0.651
5.08	6.31	16	1.00	0.730
4.66	5.67	17		0.778
4.06	4.97	18	0.988	0.792
3.51	4.26	19	0.967	0.778
2.97	3.60	20	0.895	0.736

[a] Experimental measurements of Maki et al. [26].

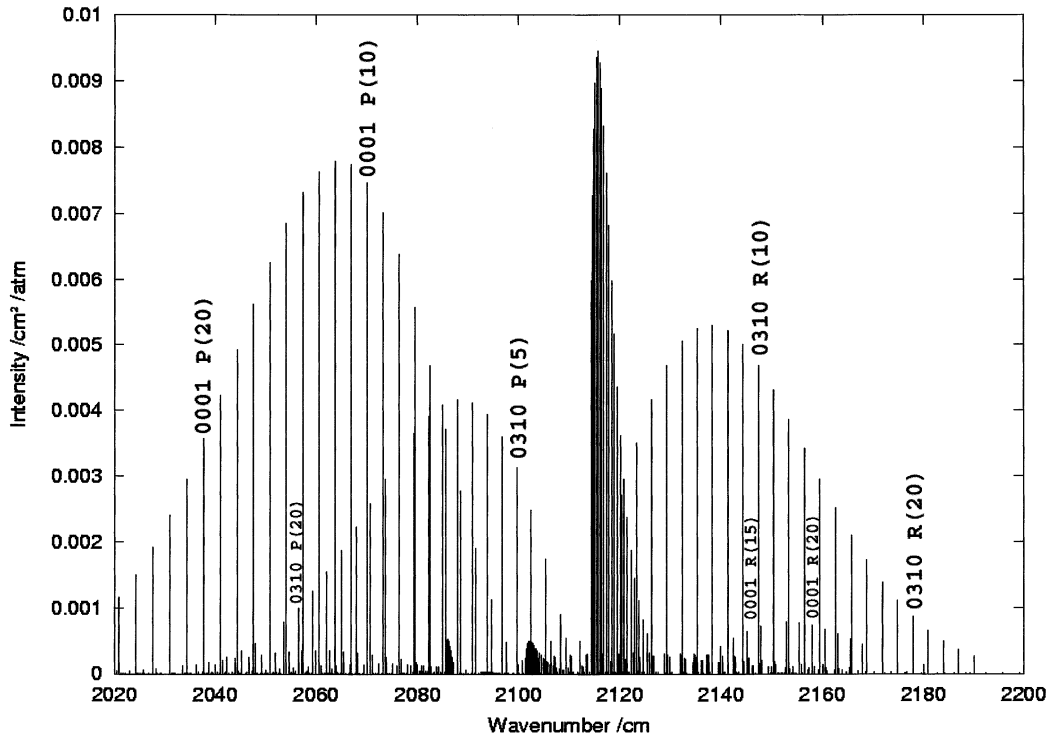

Fig. 4. The ab initio HCN absorption spectrum in the region of the HCN (00^01) fundamental at 298 K. Some lines for the P and R branches of the (00^01) fundamental and the (03^10) bend overtone are labelled.

gion of the R(15) and P(17) line. Intensity borrowing is not accounted for by Hönl-London factors, so our band intensities were calculated using lines from outside the regions in which intensity stealing was taking place. The errors on our band transition dipoles are a statistical measure of how well suited to fitting the intensity structure of a band Hönl-London factors are. For some bands, such as the ($04^{2e}0$) ← (01^10) bend hot band, errors are as much as 20%. Hönl-London factor will not accurately reproduce the intensity structure of these bands.

Table 3 compares the experimental results of Maki et al. [26] for the (00^01) band with our ab initio line intensities. The P branch ab initio line intensities are approximately 30% stronger that the experimental intensities. The ab initio R branch peak, reach minimum and peak again at $J'' = 2,8$ and 18, respectively, each of which are just above the experimental values at $J'' = 1,7$ and 16, respectively. The intensities of the R branch lines beyond the minimum ($J'' > 11$) agree well with experiment. None the less for the band our calculations are in reasonable agreement with experiment and amount to the first fully ab initio reproduction of the intensity structure of this band. The spectrum in the region of the (00^01) fundamental is plotted in Fig. 4. The P branch of the (00^01) fundamental band and the P, Q and R branches of the (03^10) overtone band are the major features in the spectrum. The unusually low intensity of the R branch of the (00^01) fundamental is clear in this figure.

Botschwina et al. [31] using wavefunctions determined from the spectroscopically fitted HCN potential surface of Carter et al. [32] and their own ab initio 110 cGTO/CCSD(T) dipole surface have calculated the band dipole for the (00^01) fundamental to within experimental error. The calculations of Botschwina et al. described the unusual structure of this band for the first time and they determined a value of $A_1 = -0.188$ for

the first order Herman–Wallis constant which agrees reasonably well with the experimentally determined value $A_1 = -0.1254$ of Maki et al. [26]. Their value of A_1, however, under predicts the position of the minimum in the R branch putting it at about $J'' = 4$ compared to the experimental value of $J'' = 7$ and our ab initio value at $J'' = 8$. This highlights the high level of sensitivity of the R branch structure to the wave functions and dipole surfaces used in the calculation.

The (02^20) bend overtone is forbidden by the normal dipole selection rules for a linear triatomic which are, for parallel transitions:

$$\Delta J = 0, \pm 1, \quad \Delta l = 0 \tag{6}$$

with $\Delta J = 0$ not allowed if $l = 0$. For perpendicular transitions:

$$\Delta J = 0, \pm 1, \quad \Delta l = \pm 1 \tag{7}$$

Some bending states with different orbital angular momentum (l) can become coupled by coriolis interactions, resulting in l being poorly defined. In this event the selection rules on l are not rigidly obeyed. The (02^20) overtone intensities we have calculated are given in Table 4, they compare well with the experimental intensities of Maki et al. [33]. The P and R branch, except for the $J'' = 5$ line, agree to within 25% of experiment and the Q branch also agrees well, to within 30% of experiment. The calculated band centre at 1432.24 cm^{-1} agrees to within 8 cm^{-1} with the experimental value from Maki et al. [34] of 1424.76 cm^{-1}.

The band centres are compared with experiment and the stretching vibrational band origins of Bowman et al. [1], in Table 2. Our calculated HCN band centres agree reasonably well with experiment, for transitions with frequency of less than 10000 cm^{-1} the mean deviation from experiment is 5 cm^{-1}, for transitions with frequency greater than 10000 cm^{-1} the mean deviation from experiment is 11 cm^{-1}. In general our stretching band centres are closer to experiment than those of Bowman et al. [1]. A fuller discus-

Table 4
A comparison of experimental and theoretical line intensities ($cm^{-2}\,atm^{-1} \times 10^{-3}$, standard deviation given in the last digit) for the HCN (02^20) forbidden overtone band

J''	P branch		R branch		Q branch	
	Experimental[a]	This work	Experimental[a]	This work	Experimental[a]	This work
2				0.000251		0.00606
3		0.00606		0.00601		0.0203
4		0.0104		0.0330		0.0442
5	0.022(8)	0.150	0.149(5)	0.106	0.061(3)	0.0785
6	0.481(8)	0.343		0.253		0.121
7	0.834(9)	0.663	0.80(2)	0.507	0.201(7)	0.171
8	1.357(21)	1.14	1.392(18)	0.890	0.252(6)	0.225
9	2.246(28)	1.77		1.41	0.291(5)	0.276
10	3.264(24)	2.56	2.899(37)	2.08	0.354(6)	0.326
11	4.445(25)	3.48	4.073(26)	2.82	0.406(6)	0.365
12	5.673(36)	4.48	5.352(25)	3.68	0.469(5)	0.397
13	7.097(36)	5.47	6.337(28)	4.52	0.455(6)	0.415
14	8.251(36)	6.41	7.447(37)	5.29	0.470(5)	0.422
15	9.141(46)	7.20	8.378(49)	5.96	0.439(7)	0.417
16	10.200(48)	7.82	8.895(47)	6.46		0.400
17	10.579(47)	8.19	9.357(52)	6.76	0.405(5)	0.375
18	10.645(79)	8.30	9.478(40)	6.83	0.390(5)	0.343
19	10.492(50)	8.17		6.70	0.346(5)	0.305
20		7.80	8.577(41)	6.32		0.266

[a] The experimental measurements of Maki et al. [33].

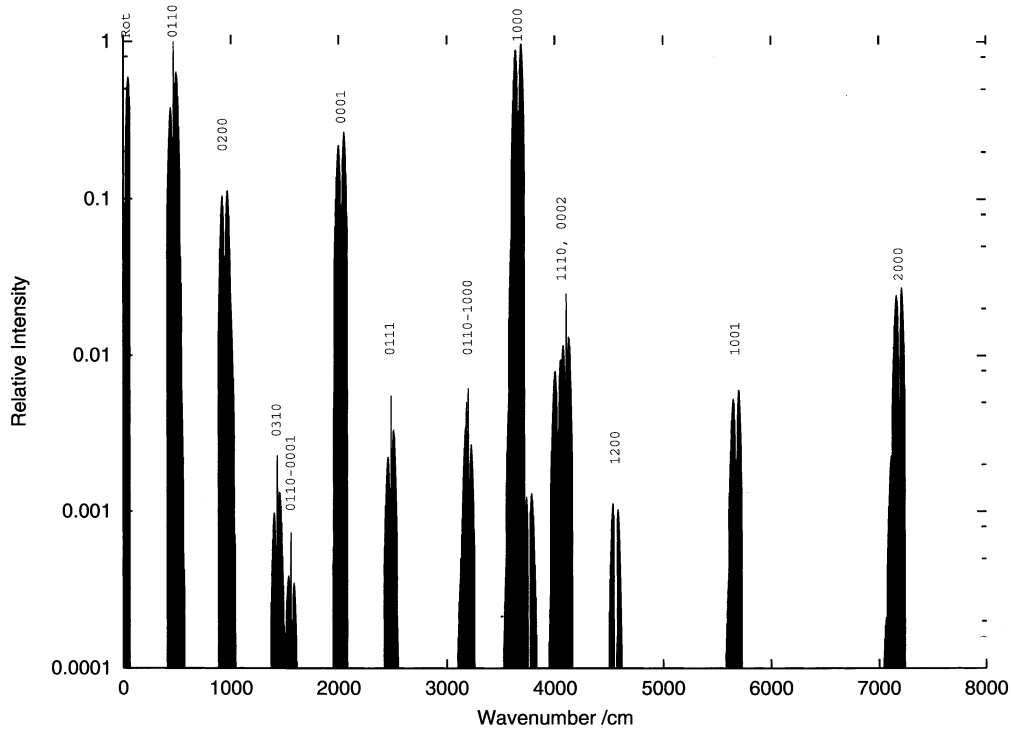

Fig. 5. Ab initio spectral atlas for HNC in absorption, between 0 and 8000 cm^{-1} at 298 K. transitions are labelled $v'_1v'_2l'v'_3$ for transitions from the ground state and $v'_1v'_2l'v'_3 - v''_1v''_2l''v''_3$ for transitions from an excited state.

sion of band origins calculated with the VQZANO + surface is given in Ref. [16].

4.2. HNC spectrum

Fig. 5 is a spectral map of room temperature (298 K) HNC in absorption, and Fig. 6 plots our spectrum against the experimental spectrum of Burkholder et al. [35] in the region of the Q and R branch of the HNC bending fundamental. The dominant features of both the experimental and ab initio spectra in Fig. 6 are the Q and R branch of the bending fundamental, but also visible are the Q branches of the bending hot bands. The Q branch of the $(02^00) \leftarrow (01^10)$ band in the experimental spectrum can just be made out within the Q branch of the bending fundamental and the Q branch of the $(02^20) \leftarrow (01^10)$ is clearly visible. The Q branches of the $(02^00) \leftarrow (01^10)$ and $(02^20) \leftarrow (01^10)$ in the ab initio spectrum at 476.794 and 481.117 cm^{-1}, respectively, are displaced from the experimental Q branches at 463.787 and 473.471 cm^{-1} due to inaccuracy of the VQZANO + potential surface. All the band transition dipoles and the band centres of the major features in the spectrum (Fig. 5) are tabulated in Tables 5 and 6.

Experimental data for band dipoles are only available for the HNC fundamentals [36,37], our ab initio calculations agree very well with both experimental and theoretical work for the stretching fundamentals. However, for the bend fundamental our calculation is in agreement with the only other theoretical value [38], but disagrees with experiment. The bending transition dipole was not directly measured by Nezu et al. [36], but determined from the transition dipoles of the stretching fundamentals using the Herman–Wallis effect. As both theoretical values agree it is likely that the value of Nezu et al. is in error, in fact Nezu et al. [37] express doubts about the accuracy of their determination of the transition dipole of the bending fundamental. Beyond the fundamen-

tal bands theoretical intensity work has been done only on the stretching overtones [2,29], our stretching overtones are in agreement with both theoretical works.

Our calculated band centres and the ab initio energy levels of Bowman et al. [1] for the CN stretching bands are of comparable accuracy, for the HN stretching bands our calculations are closer to experiment, see Table 5. Maki and Mellau [39] estimated the band centre of the ($03^{1}0$) overtone from anharmonic vibration constants of HNC up to the quartic terms which were fitted to

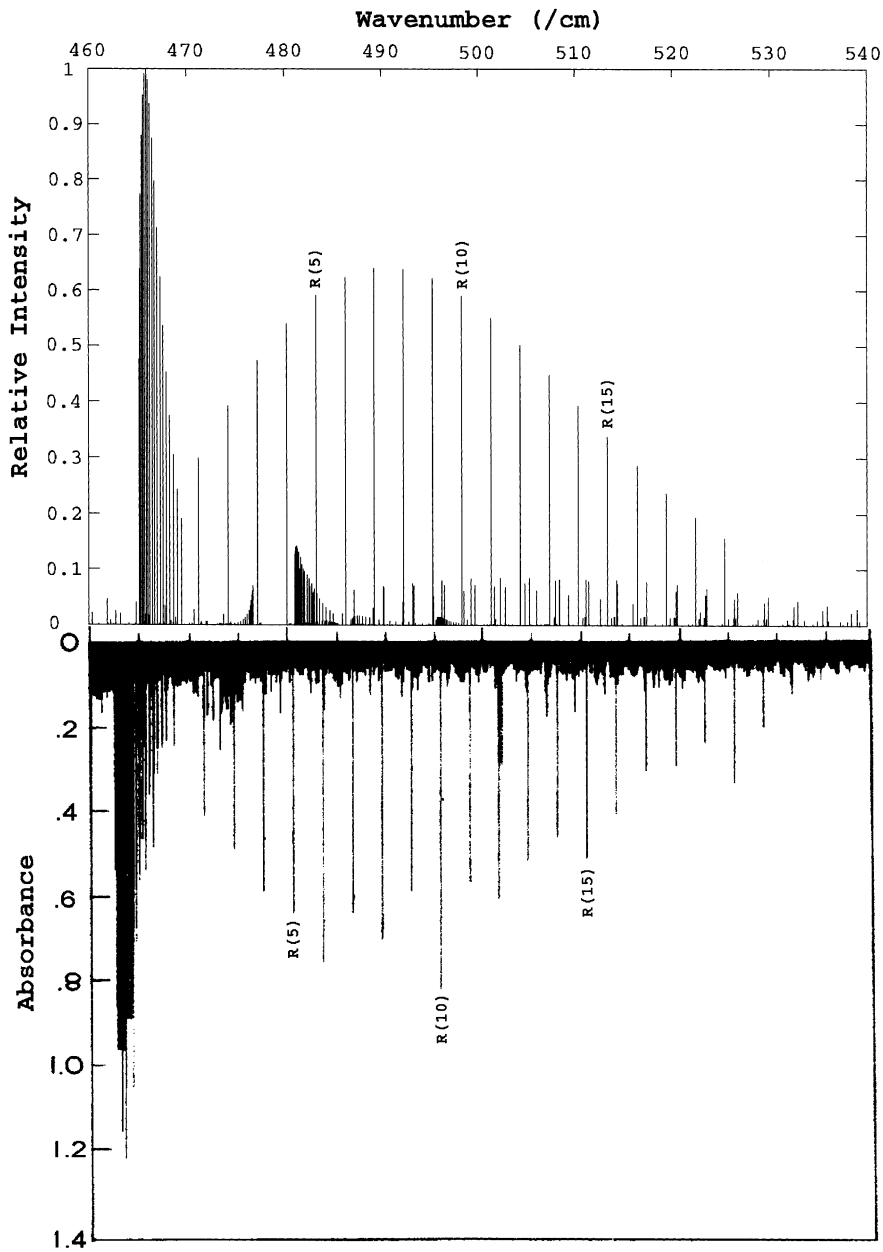

Fig. 6. A comparison of ab initio and experimental [35] absorption spectra in the region of the Q and R branch of the HNC ($01^{1}0$) fundamental at 298 K.

Table 5
A comparison of experimental and theoretical band centres (cm^{-1}) and transition dipoles (Debye, with standard deviation given in the last digit in brackets) for HNC fundamentals and some stretching overtones which are the prominent features of the spectrum at 298 K

$v'_1v'_2l'v'_3$	Experimental[a]		This work[b]		aug-cc-pVTZ[c]		Other theory		
	v_0	μ	v_0	μ	v_0	μ	v_0[d]	μ[e]	μ[f]
0 1 1 0	462.722	[1.04(27)][g]	465.190	0.463(3)					0.490
0 0 0 1	2023.86	0.108(16)	2024.94	0.104(2)	2023.9	0.106	2024.6	0.103	0.102
1 0 0 0	3652.66	0.156(23)	3665.12	0.151(2)	3652.7	0.157	3599.1	0.157	0.164
0 0 0 2	4026.40[h]		4029.20	0.0138(3)	4026.4	0.0136	4024.4	0.0126	
1 0 0 1	5664.85[h]		5676.51	0.00943(2)	5664.1	0.00999	5628.7	0.00985	
2 0 0 0	7171.40[h]		7189.53	0.0179(1)	7172.1	0.0163	7116.7	0.0134	

[a] Experimental data, band centres from Maki and Mellau [39] and Northrup et al. [46] and band transition dipoles from Nezu et al. [36,37].
[b] The ab initio calculations of this work, using the VQZANO + PES and the cc-pCVQZ/CCSD(T) DMS of van Mourik et al. [16].
[c] The ab initio stretch only cc-pVQZ/CCSD(T) potential and aug-cc-pVTZ/CCSD(T) dipole surface calculations of Botschwina et al. [29].
[d] The ab initio ANO/CCSD(T) vibrational energy level calculations of Bowman et al. [1], quoted here are stretching levels only, see text.
[e] The ab initio TZP AQCC calculations of Jakubetz and Lan [2], using the Bowman et al. [1] potential surface.
[f] The TZ2P/CCSD(T) calculations of Lee and Rendell [38].
[g] The transition dipole of the bending fundamental was estimated from the stretching fundamental transition dipoles using Herman–Walis effect by Nezu et al. [36], see text.
[h] These transitions have not been directly measured, but have been inferred from other transitions.

Table 6
A comparison of experimental and theoretical band centres (cm^{-1}) and transition dipoles (Debye, with standard deviation give to the last digit in brackets) of HNC hot bands and overtones which involve a degree of bending mode excitation and are prominent features in the spectrum at 298 K

$v'_1v'_2l'v'_3$	$v''_1v''_2l''v''_3$	Experimental[a]	This work	
		v_0	v_0	μ
0 2 0 0	0 1 1 0	463.787	476.794	0.466(154)
0 2 2 0	0 1 1 0	473.471	481.117	0.424(188)
0 2 0 0	0 0 0 0	926.507[b]	941.910	0.0976(67)
0 3 1 0	0 0 0 0	[1400.51][c]	1428.85	0.0673(77)
0 0 0 1	0 1 1 0		1559.69	0.0199(1)
0 1 1 1	0 1 1 0	2015.76	2017.54	0.103(16)
0 1 1 1	0 0 0 0	2478.48[b]	2482.67	0.0141(1)
1 0 0 0	0 1 1 0		3199.88	0.0407(16)
1 1 1 0	0 1 1 0	3630.19	3640.77	0.146(5)
1 1 1 0	0 0 0 0	4092.91[b]	4105.90	0.0227(14)
1 2 0 0	0 0 0 0	4534.45[b]	4558.15	0.00455(42)

[a] Experimental band centres from Maki and Mellau [39] and Northrup et al. [46].
[b] These transitions have not been directly measured, but have been inferred from other transitions.
[c] This band centre was estimated by Maki and Mellau [39] from anharmonic vibration constants of HNC upto the quartic terms, see text.

their experimental data with a standard deviation of 16 cm^{-1}. The large standard deviation of their fit implies that estimates of band centres from these constants will not be very accurate and as a result the large deviation from theory seen in Table 6 is to be expected. The stretching only HNC band centre calculations of Botschwina et al. [29] are in good agreement with experiment. This is despite using a 133 cGTO basis which is smaller than the cc-pCVQZ basis (198 cGTO) used for part of the VQZANO + PES [16]. However, the HNC potential of Botschwina et al. [29] considered stretching only coordinates. Experiment and the ab initio calculations of this work for the band centres of the HNC N–H stretch fundamental and overtone deviate by 12.5 and 18.0 cm^{-1}, respectively. It is likely that this deviation is caused by the cc-pCVQZ/aug-cc-pCVQZ basis not being large enough to accurately describe the electronic structure of the molecule at HNC geometries in the R coordinate.

4.3. Dipole moments

The $J = 1 \rightarrow 0$ pure rotational transition dipole calculated in this work is compared to experimental data and the ab initio vibrationally averaged dipole moments calculated by Bowman et al. [3] in Table 7. The HCN ground state and excited states for our dipole moment agree marginally less favourably with experiment than those of Bowman et al. However, for the HNC ground state we agree significantly better with observation than Bowman et al. [3], which deviates from experiment by -0.078 debye and gives a value for the HNC ground state dipole that is lower than that of the HCN ground state dipole. Botschwina et al. [31] used the empirical PES of Carter et al. [32] and a 110 GTO ab initio dipole moment surface for their calculations. Their results agree more closely with experiment than do the two fully ab initio calculations. Implying that the errors in the fully ab initio calculations are primarily due to the ab initio wavefunctions not being accurate enough.

Stanton [40] provided Bowman et al. [3] with benchmark calculations, at the cc-pCVQZ/CCSD(T) level, of the dipole moment at the three critical points of the system. The dipole moment given by the cc-pCVQZ/CCSD(T) DMS of van Mourik et al. at the geometries of the critical points calculated at the cc-pCV5Z/CCSD(T) level by van Mourik et al. [16] are given in Table 8. The dipole moments from the DMS of van Mourik et al. are in good agreement with the calculations of Stanton [40] and the dipole moment from the DMS of Bowman et al. [1].

5. Conclusions

We have computed room temperature spectra, band centres and band transition dipoles of HCN and HNC using purely ab initio techniques. Features in our spectra, including the region of the

Table 7
A comparison of experimental and theoretical vibrationally averaged dipole moments of $J = 0$ low lying HCN states and the HNC ground state

(v_1, v_2, v_3)	Experimental	aug-cc-pCVTZ[a]	cc-pCVQZ[b]	110 cGTO[c]
(0,0,0)	2.985[d]	2.9752	2.9641	2.9800
(0,2,0)	2.899[d]	2.8793	2.8776	2.8935
(0,0,1)	2.981[d]	2.9698	2.9599	2.9753
(1,0,0)	3.017[d]	3.0054	2.9961	3.0116
(0,0,0)[e]	3.05[f]	2.9721	3.0320	–

[a] Dipole moment calculations of Bowman et al. [3] with aug-cc-pCVTZ/CCSD(T) DMS.
[b] This work, $J = 0 \rightarrow 1$ rotational transition dipole using cc-pCVQZ/CCSD(T) DMS.
[c] Dipole moment calculations of Botschwina et al. [31] with HCN-only 110 cGTO/CCSD(T) DMS.
[d] Deleon and Muenter [47].
[e] HNC ground state.
[f] Blackman et al. [48].

Table 8
A comparison of ab initio dipole moments (Debye) at the three critical points

	aug-cc-pCVTZ DMS[a]	cc-pCVQZ DMS[b]	Optimised cc-pCVQZ[c]
HCN	2.999	2.993	2.994
TS[d]	1.171	1.181	1.178
HNC	−3.087	−3.121	−3.094

[a] Dipole moments from the aug-cc-pCVTZ/CCSD(T) DMS of Bowman et al. [3] at the coordinates of the critical points calculated by Stanton [40] at the cc-pCVQZ/CCSD(T) level.

[b] The Dipole moments from the cc-pCVQZ/CCSD(T) DMS of van Mourik et al. [16] at the coordinates of the critical points calculated at the cc-pCV5Z/CCSD(T) level.

[c] Dipole moment at the critical points calculated by Stanton [40] at the cc-pCVQZ level.

[d] The transition state of [H,C,N].

HCN CN stretching fundamental and the HNC bending fundamental, match well the features of HCN and HNC spectra in published figures. We have plotted and assigned bands to a HCN spectral map in the range 0–18000 cm^{-1} and to a HNC spectral map in the range 0–8000 cm^{-1}.

In general our band centres agree more closely with experiment than do the ab initio energy levels of Bowman et al. [1] calculated with their global ab initio PES. Our band transition dipoles for both HCN and HNC agree more closely with experiment than do those of the ab initio global DMS Jakubetz and Lan [2] and are of comparable accuracy to the stretching only CCSD(T) calculations of Botschwina et al. [29]. We have also reproduced the unusual structure of the HCN CN stretch fundamental via fully ab initio techniques for the first time and have calculated the intensities of the forbidden Q branch of the HCN (02^20) overtone, which compare well with experiment.

Finally our HCN $J=1\rightarrow 0$ transition dipoles compare well with experiment and also with the vibrationally averaged dipole moments of Bowman et al.

Reported here are band transition dipoles for several HCN and many HNC bands for which no experimental or computationally determined band transition dipoles have previously been reported.

An important reason for using ab initio techniques for calculating rotation–vibration is that these predictions are useful for spectral analysis. In particular the use of variational nuclear motion calculations and ab initio has provided means of assigning otherwise unanalysable spectra [41]. A key feature of this ab initio procedure, often not shown by methods which involve fitting to spectra, is that once rotational progressions can be reliably extrapolated [42]. This means that once allowance is made for the overall band error, predictions can be very reliable. The present calculations, see Fig. 6 for example, reproduce the rotational structure of the spectra accurately and will form a good starting point for further spectral analysis.

This calculation is presently being extended to the high temperatures required for astrophysical studies.

Acknowledgements

We thank Tanja van Mourik and Attila G. Császár for many helpful discussions. The calculations were performed on the Miracle 24-processor Origin 2000 supercomputer at the HiPerSPACE computing centre, UCL, which is part funded by the UK Particle Physics and Astronomy Research Council (PPARC). The UK Engineering and Physical Science Council, PPARC, the British council, the Russian Fund for Fundamental Studies, and the Hungarian–British Joint Academic and Research Programme (project no. 076) are gratefully acknowledged for funding.

References

[1] J.M. Bowman, B. Gazdy, J.A. Bentley, T.J. Lee, C.E. Dateo, J. Chem. Phys. 99 (1993) 308.
[2] W. Jakubetz, B. Leong Lan, Chem. Phys. 217 (1997) 375.
[3] J.M. Bowman, S. Irle, K. Morokuma, A. Wodtke, J. Chem. Phys. 114 (2001) 7923.
[4] W.F. Huebner, L.E. Snyder, D. Buhl, Icarus 23 (1974) 580.
[5] W.M. Irvine, D. BockeleeMorvan, D.C. Lis, H.E. Matthews, N. Biver, J. Crovisier, J.K. Davies, W.R.F. Dent, D. Gautier, P.D. Godfrey, J. Keene, A.J Lovell, T.C. Owen, T.G. Phillips, H. Rauer, F.P. Schloerb, M. Senay, K. Young, Nature 383 (1996) 418.

[6] T. Hidayat, A. Marten, B. Beźard, D. Gautier, T. Owen, H.E. Matthews, G. Paubert, Icarus 126 (1997) 170.
[7] J. Hatchell, T.J. Millar, S.D. Rodgers, Astron. Astrophys. 332 (1998) 695.
[8] T. Hirota, S. Yamamoto, H. Mikami, M. Ohishi, Ap. J. 503 (1998) 717.
[9] W. Aoki, T. Tsuji, K. Ohnaka, Astron. Astrophys. 340 (1998) 222.
[10] J.H. Bieging, S. Shaked, P.D. Gensheimer, Ap. J. 543 (2000) 897.
[11] J.H. Bieging, Ap. J. 549 (2001) L125.
[12] L.E. Snyder, D. Buhl, BAAS 3 (1971) 388.
[13] L.E. Snyder, D. Buhl, Ann. N. Y. Acad. Sci. 194 (1972) 17.
[14] K. Eriksson, B. Gustafsson, U.G. Jørgensen, Å. Nordlund, Astron. Astrophys. 132 (1984) 37.
[15] U.G. Jørgensen, J. Almlöf, B. Gustafsson, M. Larsson, P. Siegbahn, J. Chem. Phys. 83 (1985) 3034.
[16] T. van Mourik, G.J. Harris, O.L. Polyansky, J. Tennyson, A.G. Császár, P.J. Knowles, J. Chem. Phys. 115 (2001) 3706.
[17] Q. Wu, J.Z.H. Zhang, J.M. Bowman, J. Chem. Phys. 107 (1997) 3602.
[18] G. Winnewisser, A.G. Maki, D.R. Johnson, J. Mol. Spectry. 39 (1971) 149.
[19] R.A. Creswell, A.G. Robiette, Mol. Phys. 36 (1978) 867.
[20] J. Tennyson, J.R. Henderson, N.G. Fulton, Comput. Phys. Commun. 86 (1995) 175.
[21] openMP consortium, http://www.openmp.org.
[22] Silicon Graphics Inc. http://www.sgi.com/developers/nibs/1998/mipspro_apr98.html.
[23] A. Maki, W. Quapp, S. Klee, J. Mol. Spectry. 171 (1995) 420.
[24] A.M. Smith, U.G. Jørgensen, K.K. Lehmann, J. Chem. Phys. 87 (1987) 5649.
[25] W. Gordy, R.L. Cook, Microwave Molecular Spectra, 3rd ed., Wiley, New York, 1984.
[26] A. Maki, W. Quapp, S. Klee, G.Ch. Mellau, S. Albert, J. Mol. Spectry. 174 (1995) 465.
[27] A.M. Smith, W. Klemperer, K.K. Lehmann, J. Chem. Phys. 90 (1989) 4633.
[28] D. Romanini, K.K. Lehmann, J. Chem. Phys. 99 (1993) 6287.
[29] P. Botschwina, B. Schulz, M. Horn, M. Matuscheweski, Chem. Phys. 190 (1995) 345.
[30] P. Botschwina, J. Chem. Faraday Trans. 2 84 (1988) 1263.
[31] P. Botschwina, M. Horn, M. Matuscheweski, E. Schick, P. Sebald, J. Mol. Struct. (Theochem) 400 (1997) 119.
[32] S. Carter, I.M. Mills, N.C. Handy, J. Chem. Phys. 97 (1992) 1606.
[33] A. Maki, W. Quapp, S. Klee, G.Ch. Mellau, S. Albert, J. Mol. Spectry. 185 (1997) 365.
[34] A. Maki, W. Quapp, S. Klee, G.Ch. Mellau, S. Albert, J. Mol. Spectry. 180 (1996) 323.
[35] J.B. Burkolder, A. Sinha, P.D. Hammer, C.J. Howard, J. Mol. Spectry. 126 (1987) 72.
[36] M. Nezu, T. Amano, K. Kawaguchi, J. Mol. Spectry. 192 (1998) 47.
[37] M. Nezu, T. Amano, K. Kawaguchi, J. Mol. Spectry. 198 (1999) 186.
[38] T.J. Lee, A.P. Rendell, Chem. Phys. Lett. 177 (1991) 491.
[39] A. Maki, G.Ch. Mellau, J. Mol. Spectry. 206 (2001) 47.
[40] J.F. Stanton quoted by Ref. [3], see also K.L. Bak et al. J. Chem. Phys. 114 (2001) 6548.
[41] O.L. Polyansky, N.F. Zobov, S. Viti, J. Tennyson, P.F. Bernath, L. Wallace, Science 277 (1997) 346.
[42] O.L. Polyansky, N.F. Zobov, S. Viti, J. Tennyson, P.F. Bernath, L. Wallace, Astrophys. J. 89 (1997) L205.
[43] A. Maki, G.Ch. Mellau, S. Klee, M. Winnewisser, W. Quapp, J. Mol. Spectry. 202 (2000) 67.
[44] M. Lecoutre, F. Rohart, T.R. Huet, A.G. Maki, J. Mol. Spectry. 203 (2000) 158.
[45] D. Jonas, X. Yang, A. Wodtke, J. Chem. Phys. 97 (1992) 2284.
[46] F.J. Northrup, G.A. Bethardy, R.G. Macdonald, J. Mol. Spectry. 186 (1997) 349.
[47] R.L. DeLeon, J.S. Muenter, J. Chem. Phys. 80 (1984) 3892.
[48] G.L. Blackman, R.D. Brown, P.D. Godfrey, H.I. Gunn, Nature 261 (1976) 395.
[49] A.J.C. Varandas, S.P.J. Rodrigues, J. Chem. Phys. 106 (1997) 9647.